

Shearing a Glassy Material: Numerical Tests of Nonequilibrium Mode-Coupling Approaches and Experimental Proposals

Ludovic Berthier¹ and Jean-Louis Barrat²

¹CECAM, ENS-Lyon, 46, Allée d'Italie, 69007 Lyon, France

²Département de Physique des Matériaux, UCB Lyon 1 and CNRS, 69622 Villeurbanne, France

(October 29, 2018)

The predictions of a nonequilibrium schematic mode-coupling theory developed to describe the nonlinear rheology of soft glassy materials have been numerically tested in a sheared binary Lennard-Jones mixture. The theory gives an excellent description of the stress/temperature ‘jamming’ phase diagram of the system both at the microscopic and the macroscopic levels. In the present paper, we focus more particularly on the issue of an effective temperature T_{eff} for the slow modes of the fluid, as defined from a generalized fluctuation-dissipation theorem. As predicted theoretically, many different observables are found to lead to the same value of T_{eff} , suggesting several experimental procedures to measure T_{eff} . New, simple experimental protocols to access T_{eff} from a generalized equipartition theorem are also proposed, and one such experiment is numerically performed. These results give strong support to the thermodynamic interpretation of T_{eff} and make it experimentally accessible in a very direct way.

PACS numbers: 64.70.Pf, 05.70.Ln, 83.60.Df

Glassy materials are usually defined by the fact that their relaxation time is larger than the experimental time scale. In simple molecular systems, the associated glass transition temperature corresponds to very high viscosities, making it difficult to investigate experimentally their rheological properties. In complex fluids (e.g. colloids, emulsions) it is however possible to reach a glassy situation, in the sense of large relaxation times, with systems having viscosities or shear moduli that allow for rheological investigations [1]. Such materials have been described as ‘soft glassy materials’ [2].

In its glassy state, a material is by definition out of equilibrium. Physical properties are then a function of the time t_w spent in the glassy phase, a behavior called aging [3]. Interestingly, recent experiments on various complex fluids have demonstrated striking similarities with other, more standard, glassy systems [4–8]. Upon imposing a steady, homogeneous shear flow, a different kind of nonequilibrium situation is obtained. The flow, characterized by the shear rate γ , creates a *nonequilibrium steady state*, in which time translation invariance is recovered [9]. This situation can therefore be used to probe the glassy state, with the convenient feature of having the shear rate γ rather than the waiting time t_w as a control parameter. Moreover, this way of probing the nonequilibrium properties of glassy systems is probably more relevant experimentally than the aging approach, at least in the case of soft glassy materials.

Recently, a general scenario was proposed for glassy systems subject to an external forcing [10], based on the study of mean-field models. The rationale of this approach is that the equilibrium dynamics of these models is equivalent to the ‘schematic’ mode-coupling approach of slowing down in supercooled liquids [11,12].

The study of their nonequilibrium dynamics can thus be seen as a *nonequilibrium* schematic mode-coupling approach [3,13,14]. To our knowledge, the mode-coupling theory of supercooled fluid has not yet been extended to fluid under shear beyond the linear response regime. However, in analogy to what was done for aging or supercooled systems, it is sensible to bypass this aspect and to carry out a direct comparison between mean-field predictions and experimental or numerical results.

The aim of this work is thus to check on a realistic model of a fluid the predictions that emerged from the theoretical approach of Ref. [10]. Several earlier studies have been devoted to simulating glassy sheared fluids. Ref. [15] focused on the dynamics at the molecular level. Our study is devoted to more global aspects, with the aim of providing experimentally testable predictions. Ref. [16] also proposed to use the shear rate as a control parameter for jamming systems. Some dynamic aspects of a model similar to ours, with the difference of being athermal (zero temperature) have been investigated, as discussed in a companion paper [17].

We have investigated the stress/temperature jamming phase diagram (Fig. 1) of the ‘standard model’ for supercooled liquids, namely a 3D 80:20 binary Lennard-Jones mixture, in a simple shear flow defined by $\mathbf{v} = \gamma y \mathbf{e}_x$. The system consists of $N = 2916$ particles in a cubic simulation box. It has been characterized in much details at the reduced density $\rho = 1.2$, where we carry out our simulations, both in supercooled [18] and aging [19] regimes. Our simulations follow the protocol detailed in Ref. [20]: the system is first made stationary on a timescale of a few γ^{-1} . Then we perform our measurements in a range $T \in [0.15, 0.6]$ and $\gamma \in [10^{-4}, 10^{-1}]$. Standard Lennard-Jones units [18,20] are used.

Following the theoretical analysis of Ref. [10], our approach consists in three main steps. We first investigate macroscopic rheological aspects (flow curves). We then focus on microscopic properties by an analysis of the density fluctuations: structure factor, density-density correlation functions. Both aspects will be discussed in much more detail in a longer publication [21]. Last, we analyse the main new feature for the field of rheology which emerged in Ref. [10], namely the existence, behavior and properties of an effective temperature, defined through a generalized fluctuation-dissipation theorem [13]. This point, together with its experimental consequences are the main object of this paper.

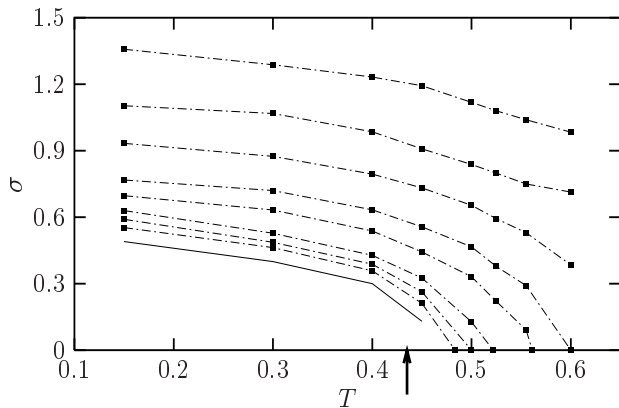


FIG. 1. The (σ, T) plane of the jamming phase diagram. The dashed curves are the viscosity contour plots with $\eta = 20, 30, 50, 100, 200, 500, 1000$ and 2000 (from top to bottom). The full line is the yield stress $\sigma_0(T)$, from Eq. (1). Arrow marks the mode-coupling temperature $T_c \simeq 0.435$.

The macroscopic behavior of the system under shear is summarized in a stress/temperature phase diagram in Fig. 1. Our results are qualitatively similar to the one reported in Ref. [15] on a different glass-former. A Newtonian behavior is observed in the high- T , low- σ part of the phase diagram. This corresponds roughly to situations where γ^{-1} is larger than the relaxation time of the fluid, which is thus only weakly affected by the flow. Outside this region, we find that the viscosity of the fluid decreases when the shear rate increases, a shear-thinning behavior reported in various ‘soft glassy materials’ [1]. We used the phenomenological relation [1]

$$\sigma \simeq \sigma_0 + a\gamma^n. \quad (1)$$

to extract the behavior of the yield stress $\sigma_0(T)$, reported in Fig. 1. This ‘jamming transition’ line was recently experimentally investigated [22]. Although our results cover 3 decades in shear rate, we cannot report a definitive functional form for the shear-thinning of the viscosity [23] which can also be satisfactorily described by

$\sigma_0 \equiv 0$, which amounts to describe the system as a power-law fluid, $\eta \sim \gamma^{n-1}$. In the supercooled regime we find $n \simeq 1/3$, while at lower temperatures, the exponent n is temperature dependent with $n \rightarrow 0$ when $T \rightarrow 0$, indicating that a yield stress could exist in this limit only [21]. The latter power-law behavior is precisely the one predicted theoretically in Ref. [10].

Equilibrium mode-coupling theory gives rise to several quantitative predictions regarding the scaling properties of the intermediate scattering function,

$$C_{\mathbf{k}}(t) = \frac{1}{N} \sum_{j=1}^N \langle \exp(i\mathbf{k} \cdot [\mathbf{r}_j(t+t_0) - \mathbf{r}_j(t_0)]) \rangle, \quad (2)$$

when the glassy phase is approached by lowering T with $\sigma = 0$. It was shown in Ref. [10] that similar scaling properties are expected when the glassy phase is approached by lowering the shear stress σ at constant temperature (vertical line in Fig. 1). We have tested in a detailed way these predictions in our simulation [21]. Here, we only report the validity of the theoretically predicted ‘time-shear superposition property’ [10] in Fig. 2, which shows that the slow decay of $C_{\mathbf{k}}(t)$ has the scaling form $C_{\mathbf{k}}(t) \simeq F(t/t_{\text{rel}})$, where the relaxation time is defined, as usual, by $C_{\mathbf{k}}(t_{\text{rel}}) \equiv e^{-1}$. The scaling function $F(x)$ is well described by a stretched exponential, $F(x) \sim \exp(-x^\beta)$, with an exponent β which increases from $\beta \sim 0.77$ for $T \gtrsim T_c$ to the value $\beta = 1$ as $T \rightarrow 0$.

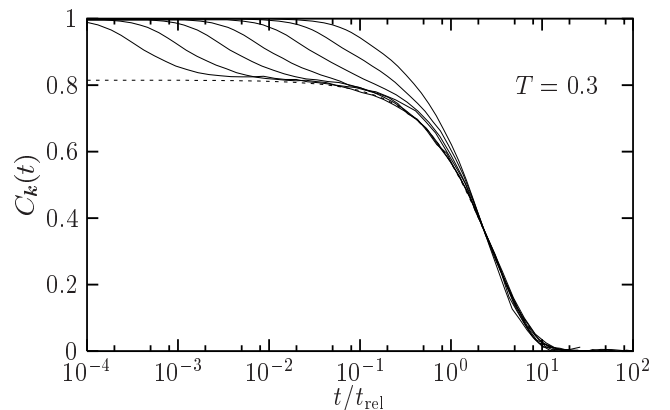


FIG. 2. Correlation functions for $T = 0.3 < T_c$ and different values of the shear rate, $\gamma = 10^{-4}, 3 \cdot 10^{-4}, 10^{-3}, 3 \cdot 10^{-3}, 10^{-2}, 3 \cdot 10^{-2}, 10^{-1}$ (from left to right at $C = 0.9$) can be collapsed if the time is rescaled by $t_{\text{rel}}(\gamma)$. The dashed line is a fit to a stretched exponential form, with an exponent $\beta = 0.95$.

We now focus on the issue of an effective temperature for the slow modes of the sheared fluid. This quantity, naturally included in nonequilibrium mode-coupling theories [10], is defined through a nonequilibrium generalization of the fluctuation-dissipation theorem (FDT) [13].

Consider two physical observables, $O(t)$ and $O'(t)$, their connected cross-correlation function $C_{OO'}(t) \equiv \langle O(t+t_0)O'(t_0) \rangle - \langle O(t_0) \rangle \langle O'(t_0) \rangle$, and the response function $R_{OO'}(t) \equiv \frac{\delta \langle O(t+t_0) \rangle}{\delta h_{O'}(t_0)}$, where $h_{O'}$ is the field thermodynamically conjugated to $O'(t)$. At equilibrium, both quantities satisfy the FDT, $TR_{OO'}(t) = \frac{dC_{OO'}(t)}{dt}$. The susceptibility $\chi_{OO'}(t) \equiv \int_0^t dt' R_{OO'}(t')$ can be measured by applying a small (to ensure linear response), constant field $h_{O'}$ between times 0 and t and FDT implies a simple linear relation $T\chi_{OO'}(t) = (C_{OO'}(0) - C_{OO'}(t))$. In the sheared fluid, an effective temperature is *defined* by

$$R_{OO'}(t) = -\frac{1}{T_{\text{eff}}^{OO'}(C_{OO'})} \frac{dC_{OO'}(t)}{dt}, \quad (3)$$

where the $T_{\text{eff}}^{OO'}(x)$ are *a priori* arbitrary functions of their argument, which may in general depend on the observables O and O' under study. For any pair of observables, $T_{\text{eff}}^{OO'}(x)$ can be measured in the sheared system, by following the same linear response procedure as above, so that $\chi_{OO'}(t) = \int_0^{C_{OO'}(0)} \frac{dx}{T_{\text{eff}}^{OO'}(x)}$. The existence of an effective temperature is thus *demonstrated* if a straight line is obtained in a susceptibility-correlation plot parameterized by the time. Obviously, the introduction of an effective temperature is of ‘thermodynamic’ interest only if this quantity is actually independent of the observables under consideration, $T_{\text{eff}}^{OO'} \equiv T_{\text{eff}}$. This crucial feature is true at the mean-field level [13,14], and we shall prove that it is nicely satisfied in our model.

We have already shown the existence of such an effective temperature for the slow modes of the system for a single correlation function, Eq. (2), at a given wavevector [20]. We also found that the essential phenomenological idea that a system sheared more vigorously has a higher T_{eff} is indeed captured by this definition [20].

Here, we go much further in our investigations and prove that several different observables lead to the same value of T_{eff} . Since the numerical measurement of T_{eff} is very demanding, our strategy has been to compute for $T = 0.3$ and $\gamma = 10^{-3}$ the value of T_{eff} from the observables of Ref. [20] with a great accuracy. We found $T_{\text{eff}} \simeq 0.65$. We then computed T_{eff} using different observables, and checked that the value so obtained was compatible with $T_{\text{eff}} = 0.65$. Our results are summarized in Fig. 3 which shows 10 among the 14 different susceptibility-correlation measurements we have performed. All our data are well compatible with the single value of $T_{\text{eff}} = 0.65$ for the slow modes of the fluid.

We first investigated the density fluctuations as an observable, taking $O(t) = \frac{1}{N} \sum_{j=1}^N \varepsilon_j \exp(i\mathbf{k} \cdot \mathbf{r}_j(t))$, and $O'(t) = 2 \sum_{j=1}^N \varepsilon_j \cos(\mathbf{k} \cdot \mathbf{r}_j(t))$. For some wavevectors, this was done separately for both types (A and B) of Lennard-Jones particles (noted ‘ $A+B$ ’ in Fig. 3). Taking $\varepsilon_j = 1$ selects the coherent part of the intermediate scattering function (noted ‘coh’ in Fig. 3), while $\varepsilon_j = \pm 1$ se-

lects the incoherent one. Such response-correlation plots could be obtained experimentally in soft condensed matter systems. While the correlation functions are reasonably easily obtainable through light scattering experiments, the same is not true of response functions. To obtain the latter, one has to manipulate the particles through some externally applied potential, modulated at the same wavevector as used in the light scattering experiment. One suggestion would be to use some non-index matched tracer particles in an index matched colloidal suspension. The tracer particles would then be sensitive to the intensity of the local electric field, as in optical tweezers. An interference pattern would actually realize the modulated external potential considered here. Reading of the response could then be obtained from the scattering at the wavelength corresponding to this pattern.

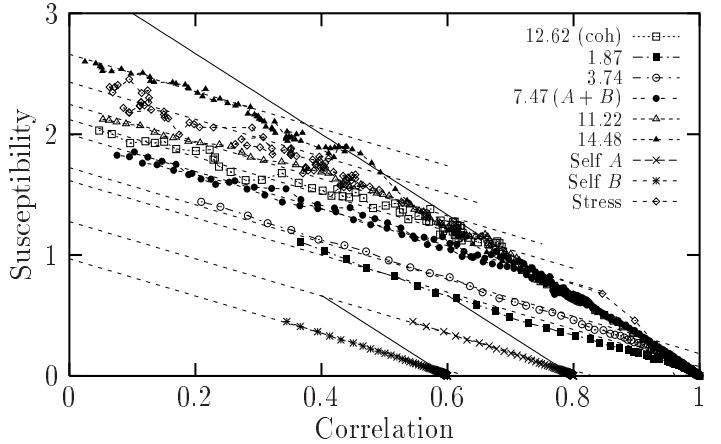


FIG. 3. Ten representative susceptibility-correlation plots are shown to be consistent with the same T_{eff} for the slow modes (small value of the correlation). Full lines are the equilibrium FDT of slope $-1/T$, dashed lines have slope $-1/T_{\text{eff}}$ with $T_{\text{eff}} = 0.65$. Numbers refer to wavevectors (see also the text).

We also used as a correlation the mean square displacement of a tagged particle. The associated response function is the displacement induced by applying a small, constant external force to this tagged particle [24]. Both quantities are linked by a FDT, the Einstein relation. We computed both quantities separately for particles of type A and B (noted ‘Self A ’ and ‘Self B ’ respectively). Its interest, especially in view of experimental realizations, lies in the fact that the full time dependence of the correlation and response functions is not needed to extract T_{eff} . Indeed, at large times, both quantities become proportional to the time which defines the diffusion constant and the mobility. One may therefore define T_{eff} simply as the ratio of diffusion to mobility. Again, experiments could be considered if tracer particles sensitive to an external force field (e.g. magnetic particles) could be introduced into the system, and their mobility measured

together with their diffusion constant.

A completely different observable, relevant to flow situations, is the stress σ . We have studied the case in which the observables O and O' are equal to the diagonal stress in the direction transverse to the flow, $\sigma_{zz}(t)$. To add a field conjugated to σ_{zz} , a compression δL_z of the simulation box is realized by rescaling all particle coordinates at time $t = 0$, in analogy to stress relaxation experiments. The corresponding curve is labelled ‘Stress’ in Fig. 3. Experimentally, the off-diagonal component of the stress would be used as the observable. Preliminary results in this direction, using an extremely sensitive rheometer, have been obtained in aging colloidal systems [25].

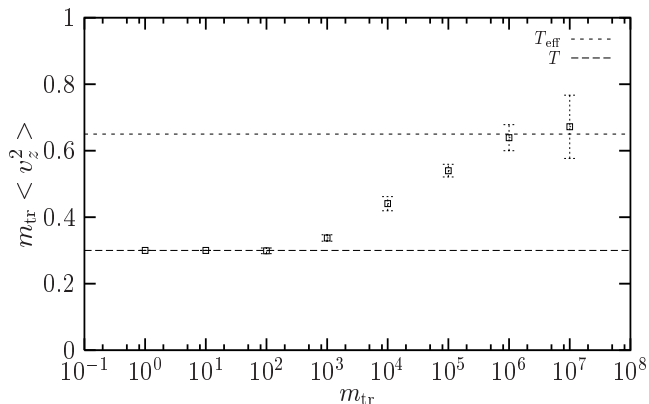


FIG. 4. Mass dependence of the mean kinetic energy in the z direction for $T = 0.3$ and $\gamma = 10^{-3}$. Horizontal lines are $T = 0.3$ and $T_{\text{eff}} = 0.65$. Error bars are evaluated from tracer to tracer fluctuations.

Definition (3) of T_{eff} implies that, if the fluid is used as a thermal bath to equilibrate a subsystem (a ‘thermometer’) of typical time scale $t_s \sim t_{\text{rel}}$, the thermometer does not measure the microscopic temperature, but rather the effective temperature associated with its characteristic time scale [13]. We propose here to use tracers of mass m_{tr} as a thermometer, since tuning m_{tr} allows to control their vibration time scale t_s . We have considered 10 massive tracers with $m_{\text{tr}} \in [1, 10^7]$, but being otherwise identical to A particles. Since $t_s \sim \sqrt{m_{\text{tr}}}$, heaviest particles have a frequency typically 10^3 times smaller than the light ones, implying $t_s \sim t_{\text{rel}}$. Reading of the temperature is done by measuring the average mean square velocity of the tracers in the direction z . Results are shown in Fig. 4, which shows that light particles measure the bath temperature while heaviest particles measure T_{eff} . This implies that a *generalized equipartition theorem* holds,

$$\left\langle \frac{1}{2} m_{\text{tr}} v_z^2 \right\rangle = \frac{1}{2} T_{\text{eff}}. \quad (4)$$

This result could be tested against experiments involving for instance colloidal particles, the tracers, in a complex

fluid, e.g. polymeric, or by investigating rotational degrees of freedom of non-spherical tracer particles.

This last result opens the way for new, simple determinations of T_{eff} in out of equilibrium glassy materials. Indeed, no ‘complex’ dynamic functions such as correlations or susceptibilities are needed here. In this context, it would be interesting to reproduce Perrin’s experiment on barometric equilibrium of colloidal suspensions [26]. We expect indeed that the barometric equilibrium of heavy particles inside a horizontally sheared fluid should be ruled by T_{eff} instead of the room temperature.

All these results give strong support to the theoretical scenario elaborated from mean-field theories to describe the rheology of soft glassy materials [10]. Note in particular that T_{eff} , which we have shown to be a physically relevant quantity, is a natural outcome of the theory. While numerical simulations provide a test of the theory on short time scales, systematic experiments that could test quantitatively existing theories of nonequilibrium glassy dynamics are still needed. In that sense, the situation is more or less similar to the mid-eighties when schematic equilibrium mode-coupling were already derived, but with little experimental confirmation of its main features. This is why we tried, as much as possible, to suggest experimental counterparts to our numerical measurements. We hope that our findings and suggestions will motivate further experimental work in the field.

We thank L. Bocquet, J. Kurchan and W. Kob for discussions. This work was supported by the PSMN at ENS Lyon and the CDCSP at Université de Lyon.

-
- [1] R. G. Larson, *The structure and rheology of complex fluids* (Oxford University Press, New York, 1999).
 - [2] P. Sollich *et al.*, Phys. Rev. Lett. **78**, 2020 (1997).
 - [3] J.-Ph. Bouchaud, L. F. Cugliandolo, J. Kurchan and M. Mézard, in *Spin glasses and random fields*, Ed.: A. P. Young (World Scientific, Singapore, 1998).
 - [4] L. Cipelletti *et al.*, Phys. Rev. Lett. **84**, 2275 (2000).
 - [5] M. Cloitre *et al.*, Phys. Rev. Lett. **85**, 4819 (2000).
 - [6] L. Ramos and L. Cipelletti, Phys. Rev. Lett. **87**, 245503 (2001).
 - [7] A. Knaebel *et al.*, Europhys. Lett. **52**, 73 (2000).
 - [8] C. Dérec *et al.*, Faraday Discuss. **112**, 195 (1999).
 - [9] L. F. Cugliandolo, J. Kurchan, P. Le Doussal and L. Peliti, Phys. Rev. Lett. **78**, 350 (1997).
 - [10] L. Berthier, J.-L. Barrat and J. Kurchan, Phys. Rev. E **61**, 5464 (2000).
 - [11] T. R. Kirkpatrick and D. Thirumalai, Phys. Rev. B **36**, 5388 (1987).
 - [12] W. Götzke and L. Sjögren, Rep. Prog. Phys. **55**, 241 (1992).
 - [13] L.F. Cugliandolo, J. Kurchan and L. Peliti, Phys. Rev. E **55**, 3898 (1997).

- [14] L. F. Cugliandolo and J. Kurchan, Phys. Rev. Lett. **71**, 173 (1993); L. F. Cugliandolo, J. Kurchan, and P. Le Doussal, Phys. Rev. Lett. **76**, 2390 (1996).
- [15] R. Yamamoto and A. Onuki, Phys. Rev. E, **58**, 3515 (1998).
- [16] A. J. Liu and S. R. Nagel, Nature **396**, 21 (1998).
- [17] I. K. Ono *et al.*, submitted to Phys. Rev. Lett.
- [18] W. Kob and H. C. Andersen, Phys. Rev. E **53**, 4134 (1995); Phys. Rev. E **51**, 4626 (1995).
- [19] W. Kob and J.-L. Barrat, Eur. Phys. J. B **13**, 319 (2000).
- [20] J.-L. Barrat and L. Berthier, Phys. Rev. E **63**, 012503 (2001).
- [21] L. Berthier and J.-L. Barrat (to be published).
- [22] V. Trappe *et al.*, Nature **411**, 772 (2001).
- [23] Smaller shear rates, corresponding to larger time scales are presently numerically unreachable.
- [24] G. Parisi, Phys. Rev. Lett. **79**, 3660 (1997).
- [25] L. Bellon and S. Ciliberto, cond-mat/0201224.
- [26] J. Perrin, Annales de Chimie et Physique **18**, 1 (1909).